KI REPORTS
KIReports.org
TRANSLATIONAL RESEARCH

Establishing a Case for Anti-complement Therapy in Membranous Nephropathy

Check for updates

Isabelle Ayoub[1], John P. Shapiro[1], Huijuan Song[1], Xiaolan Lily Zhang[1], Samir Parikh[1], Salem Almaani[1], Sethu Madhavan[1], Sergey V. Brodsky[2], Anjali Satoskar[2], Cherri Bott[2], Lianbo Yu[3], Michael Merchant[4], John Klein[4], Juan M. Mejia-Vilet[5], Tibor Nadasdy[2], Dan Birmingham[1] and Brad H. Rovin[1]

[1]Department of Medicine, Division of Nephrology, The Ohio State University Wexner Medical Center, Columbus, Ohio, USA; [2]Department of Pathology, The Ohio State University Wexner Medical Center, Columbus, Ohio, USA; [3]Center for Biostatistics, The Ohio State University Wexner Medical Center, Columbus, Ohio, USA; [4]Department of Medicine, Division of Nephrology and Hypertension, University of Louisville School of Medicine, Louisville, Kentucky, USA; and [5]Department of Nephrology and Mineral Metabolism, Instituto Nacional de Ciencias Médicas y Nutrición Salvador Zubirán, Mexico City, Mexico

Introduction: Membranous nephropathy (MN) is a common cause of adult nephrotic syndrome that progresses to end-stage kidney disease in up to 40% of cases. It is an autoimmune disease characterized by glomerular subepithelial deposits containing IgG. In experimental MN, these deposits activate complement and cause kidney damage. The role of complement in human MN is less clearly defined. To address this, the current study focused on the role of complement in 2 independent primary (p) MN cohorts.

Methods: Glomeruli were isolated by laser capture microdissection and analyzed by mass spectrometry, focusing on complement proteins, from kidney biopsy specimens from a pMN cohort (n = 11) and from normal controls (n = 5). Immunohistological staining of kidney biopsy specimens for complement proteins was also done. In a second pMN cohort (n = 13), urine levels of Ba, C5a, and C5b-9 (membrane attack complex [MAC]) were measured.

Results: Mass spectrometry identified 8 complement pathway components (C1q, C3, C4, C5, C6, C7, C8, and C9) and 5 complement regulators (complement receptor type 1 [CR1], factor H [FH], FH-related protein 2 [FHR2], vitronectin, and clusterin). All complement levels were significantly higher in the MN groups than in the control group, except the level of CR1, which was lower. All pMN biopsy specimens showed negative or trace staining for C1q, positive staining for C3 and C4, and positive staining for at least 1 component of the lectin pathway. Urine Ba, C5a, and MAC were present in pMN, and their levels correlated ($r_{Ba,C5a} = 0.87$, $r_{Ba,MAC} = 0.89$, and $r_{C5a,MAC} = 0.97$, $P = .001$ for each correlation).

Conclusion: Elevated glomerular levels of C3, C4, and components of MAC (C5b-9) and absent or decreased levels of the complement regulator CR1, along with increased levels of complement activation products in the urine, support the involvement of complement in the pathogenesis of MN. These data raise the possibility that anti-complement therapies may be effective in some forms of MN.

Kidney Int Rep (2021) **6,** 484–492; https://doi.org/10.1016/j.ekir.2020.11.032
KEYWORDS: complement protein; membranous nephropathy; proteomic analysis
© 2020 International Society of Nephrology. Published by Elsevier Inc. This is an open access article under the CC BY-NC-ND license (http://creativecommons.org/licenses/by-nc-nd/4.0/).

Membranous nephropathy (MN) is a common cause of adult nephrotic syndrome that progresses to end-stage kidney disease in up to 40% of cases.[1,2] It is an autoimmune noninflammatory disease characterized by glomerular subepithelial immune complex deposits. In primary (p) MN, podocyte antigens serve as targets for circulating autoantibodies. These antigens so far include M-type phospholipase A2 receptor (PLA2R),[3] thrombospondin type-1 domain-containing 7A (THSD7A),[4] found in 70% to 80% and in 1% to 5% of cases, respectively. The most recently identified antigen, neural epidermal growth factor-like 1 protein (NELL-1),[5] is found in pMN and also in malignancy-associated MN, where it is detected more frequently than PLA2R-negative,THSD7A positivity.[6] The subepithelial immune deposits in pMN are predominantly IgG4 subclass. In contrast, MN secondary to other diseases usually has more abundant deposits of IgG1, IgG2, and IgG3 than IgG4,[7–10] and other podocyte antigen targets such as exostosin 1 (EXT1) and exostosin 2 (EXT2).[11]

Correspondence: Isabelle Ayoub, Nephrology Division, Ohio State University, Ground Floor, 395 West 12th Avenue, Columbus, Ohio 43210, USA. E-mail: Isabelle.ayoub@osumc.edu

Received 14 September 2020; revised 29 October 2020; accepted 19 November 2020; published online 13 December 2020

Table 1. Patient characteristics at the time of kidney biopsy

MS cohort	MN type	Sex	Race	Age, yr	Serum creatinine, mg/dl	eGFR, ml/min per 1.73 m^2[a]	Serum PLA2R, RU/ml[b]	Urine PCR	Sclerosed glomeruli/total glomeruli	IFTA (%)
1	IgG1	F	W	74	0.7	>60	NA	4.9	1/16	20
2	IgG1	M	W	65	1.4	52	NA	6.8	11/22	40
3	IgG1	F	W	59	0.9	>60	NA	11.3	7/18	40
4	IgG1	F	W	48	1.7	35	NA	6.0	7/21	40
5	IgG1	M	W	41	NA	NA	NA	4.4	1/32	20
6	IgG1	M	W	75	NA	NA	NA	5.0	0/8	5
7	IgG1	M	W	63	1.0	>60	NA	2.6	2/24	30
8	IgG4[c]	M	NA	69	1.7	NA	NA	3.3	0/11	25
9	IgG4[c]	M	NA	52	2.2	NA	NA	Nephrotic range[d]	2/30	30
10	IgG4[c]	M	W	19	0.8	>60	NA	5.5	1/37	0
11	IgG4	M	W	55	4.2		NA	17.0	8/23	60
Urine cohort										
Healthy control	Not done	M	W	63	0.9	>60	Not done	0.00	Not done	Not done
Healthy control	Not done	M	W	23	NA	NA	Not done	0.00	Not done	Not done
1	IgG4[c]	M	W	50	1.5	54	NA	10.0	3/41	35
2	IgG4[c]	M	W	69	0.8	>60	NA	4.0	2/16	10
3	IgG4[c]	M	W	49	1.0	>60	<14	2.6	0/10	20
4	IgG4[c]	M	W	58	1.0	>60	NA	5.8	0/16	3
5	IgG4[c]	M	W	59	0.8	>60	NA	5.8	5/24	15
6	IgG4/IgG1[c]	M	W	36	0.8	>60	NA	2.4	1/4	5%
7	IgG4/IgG1	F	W	64	0.7	>60	<14	2.2	1/5	10
8	IgG4/IgG1[c]	M	W	49	3.1	22	NA	11.0	0/15	0
9	IgG4/IgG1[c]	M	W	46	3.0	24	NA	5.7	15/21	70
10	IgG4/IgG1[c]	M	AA	56	1.0	>60	<14	2.8	2/12	5
11	IgG4/IgG1	M	W	68	1.1	>60	<14	5.8	0/16	10
12	IgG1	M	W	80	1.3	52	NA	4.0	7/21	20
13	IgG1[c]	M	W	63	1.0	>60	NA	2.5	2/24	25

AA, African American; eGFR, estimated glomerular filtration rate; F, female; IFTA, interstitial fibrosis and tubular atrophy; M, male; MN, membranous nephropathy; MS, mass spectrometry; NA, not available; PCR, urine protein-to-creatinine ratio; PLA2R, phospholipase A2 receptor; W, White.
[a]eGFR calculated using Chronic Kidney Disease Epidemiology Collaboration equation.
[b]Most of the kidney biopsy specimens were analyzed before the serum PLA2R testing became commercially available.
[c]PLA2R-positive on glomerular staining.
[d]Nephrotic range: absolute ratio was not available.

In experimental MN, antigen–antibody deposits activate complement and cause kidney damage and proteinuria.[12] In humans, glomerular staining for C3 without C1q is prominent along with IgG in pMN.[12] Given the emerging experience and clinical use of therapeutic complement inhibitors, and to further our understanding of the role of the complement system and complement pathways in pMN, we performed a proteomic study of glomeruli from kidney biopsy tissue of patients with pMN, and focused the analysis on complement proteins.

METHODS

Study Design

This study investigated patients with active pMN. Complement protein levels in the glomeruli of these biopsy specimens were investigated and compared to those of normal tissue from pre-implantation biopsy specimens of living donor kidneys.

Patients and Kidney Biopsies

Eleven patients with a kidney biopsy diagnosis of MN without an obvious secondary cause despite extensive workup were included (Table 1). Using mass spectrometry (MS), complement protein levels were measured by an unbiased approach in the kidney biopsy specimens of 4 patients with IgG4-dominant MN (3 were PLA2R-positive and 1 was PLA2R-negative by glomerular staining), and 7 patients with IgG1 dominant, PLA2R negative–MN. Normal kidney tissue from preimplantation living donor kidney biopsy specimens was used as control (n = 5). To mirror the MS findings, immunohistological staining for complement components was performed on those 11 kidney biopsy specimens. To look for evidence that the increased

abundance of complement proteins in glomeruli of patients with pMN was associated with intrarenal complement activation, urine from a second cohort of patients with active pMN (n = 13) was collected at the time of their kidney biopsy and tested for levels of urine Ba (uBa), urine C5a (uC5a), and urine membrane attack complex (uMAC) (Table 1). These patients had primary MN as suggested by the absence of obvious secondary causes, and by dominant (n = 5; all were PLA2R-positive by glomerular staining) or co-dominant (n = 6; 4 were PLA2R-positive by glomerular staining) IgG4 glomerular immunofluorescence. Two patients had only IgG1 glomerular immunofluorescence, but no underlying etiology was found in either case. Urine from 2 healthy subjects was used as control.

The investigation of the kidney biopsy specimens and the urine studies were approved by the Ohio State Institutional Review Board and performed retrospectively using archived samples.

Tissue Extraction and Analysis

Sample Preparation for Laser Capture Microdissection

Sections from paraffin blocks were cut at 10 μm and wet-mounted on Zeiss PEN membrane slides in a protease-free container with mass spectrometry grade water at 42 °C. Sections on slides were completely dried for 1 week in a desiccator under vacuum seal. Dried sections were deparaffinized and stained in a Lock-Mailer microscope mailer and staining jars (Ted Pella, Redding, CA) using the following procedure and keeping slides hydrated at all times: (i) 3 changes of octane, followed by 3 changes of 200 proof ethanol; (ii) single changes in 90% and 70% ethanol (made with mass spectrometry grade water); and then finally (iii) 2 changes of mass spectrometry–grade water. All steps were performed for 2 minutes each. Sections were briefly stained with hematoxylin (Vector Laboratories, Burlingame, CA) for 3 seconds, followed by immediate washes in 2 changes of mass spectrometry grade water. Sections were then treated with 2-minute changes each in 70%, then 90% ethanol, followed by 2 each 2-minute changes in 100% ethanol. Slides were removed from ethanol and air dried for laser capture microdissection.

Laser Capture Microdissection

Laser capture microdissection was performed using the laser microdissection system from PALM Technologies (Carl Zeiss Micro Imaging GmbH, Munchen, Germany) containing a PALM MicroBeam and RoboStage for high-throughput sample collection and a PALM RoboMover (PALM Robo software, version 2.2, Carl Zeiss, Microimaging GmbH, Munchen, Germany). Typical settings used for laser cutting were UV-Energy of 70 to 75 and UV-Focus of 80. Sections were cut and captured under a ×10 ocular lens. Cut elements were catapulted into 25 μl of 0.5% Rapigest (Waters Corporation, Milford, MA) resuspended in 50 mM NH_3HCO_3. The total number of cells captured was determined presuming that each collected glomerulus contained 200 cells. Upon completion of microdissection, the captured material was spun down into a 0.2 ml PCR tube and held at −80 °C until protein retrieval.

Protein Extraction and Digestion

Samples that had been stored at −80 °C were thawed briefly and boiled for 20 minutes, followed by a 2-hour incubation in a 60 °C water bath for protein recovery. Trypsin was added in a ratio of 1:30 (no. V511A; Promega, Madison, WI) assuming ∼ 2 μg retrieved protein/10,000 isolated cells. After overnight incubation at 37 °C, formic acid was added to a final concentration of 30% to 40% until the solution clouded after a 1-minute room temperature incubation. This suspension was incubated for 30 minutes at 37 °C to completely precipitate the Rapigest. The samples were centrifuged 3 times at 15,000 rpm at 4 °C for 10 minutes to eliminate cellular debris and the precipitated Rapigest from the sample. The extracts were dried in a speedvac. The dried peptides were resuspended in 20 μl solution of 2% acetonitrile with 0.1% formic acid, and the samples were sonicated for 1 minute in a water bath sonicator at 4 °C to ensure peptide solubilization. Final peptide concentrations were controlled by measurement of 280 nm absorbance to obtain peptide concentration in the tryptic digest on a Nanodrop ND-1000 spectrometer (Thermo Fisher, Waltham, MA).

Mass Spectrometry

Analysis Parameters

Tandem mass spectra were analyzed against a Human Ref160309 database annotated with the database for common affinity purification contaminates (CRAPome) for a tryptic digest.

Mascot and Sequest were searched with a fragment ion mass tolerance of 1.00 Da and a parent ion tolerance of 50 ppm. Carbamidomethyl of cysteine was a fixed modification. Oxidation of methionine and proline were specified as variable modifications.

Scaffold (version Scaffold_4.5.1, Proteome Software Inc., Portland, OR) was used to validate mass spectrometry (MS)/mass spectroscopy (MS)−based peptide and protein identifications. Peptide identifications were accepted if they could be established at greater than 99.9% probability by the Scaffold Local false discovery rate algorithm and contained at least 1 identified peptide. Protein probabilities were assigned by the Protein Prophet algorithm.[13] Proteins that contained similar

peptides and could not be differentiated based on MS/MS analysis alone were grouped to satisfy the principles of parsimony. Proteins sharing significant peptide evidence were grouped into clusters.

Data were filtered using a peptide mass accuracy of ≤2 ppm, minimum peptide length of 7 amino acids, 1% protein false discovery rate, and a peptide confidence interval of 99.9%. Protein abundance data were exported into Microsoft Excel (Microsoft Corporation, Redmond, WA) using measures of label-free quantification: MS2 method term Total Spectral Counts (TSC).

Technical Replicates

When possible, samples were analyzed as technical duplicates, and duplicate data were averaged at the protein level. If a protein was detected in 1 sample alone, then that value was retained without averaging.

Immunohistological Staining (MS Cohort)

Immunofluorescence was performed on sections of frozen tissue and paraffin-embedded tissue after antigen retrieval. Antigen retrieval for PLA2R was performed on paraffin-embedded tissue by using Dako/Agilent Target Retrieval (catalog no. S1699, Agilent, Santa Clara, CA) using the Pascal pressure cooker for 20 minutes. The antibodies used for the studies and their dilutions are listed in Supplementary Table S1. Antibody staining for PLA2R was done using the following protocol: serum-free protein block (catalog no. X0909, Agilent, Carpinteria, CA) for 15 minutes at room temperature; incubation with a primary antibody for 1 hour at room temperature; washing in phosphate-buffered saline solution 3 times for 5 minutes each; incubation with a secondary antibody for 30 minutes at room temperature; and washing in phosphate-buffered saline solution 3 times for 5 minutes each. Immunofluorescence for IgG1, IgG4, C1q, C3, C4d, M-Ficolin, L-Ficolin, MASP1, MASP2, and C5b-9 was performed on frozen sections cut at 4 μm and fixed in cold acetone for 10 minutes. After air drying, the slides were stained on the Biocare Intellipath. The slides were rinsed with Tris-buffered saline solution, pH 7.6 (prepared in house), for 5 minutes. The slides were then incubated in the appropriate antibody for 1 hour, rinsed in Tris-buffered saline solution, and coverslipped using an aqueous mounting medium. The slides were analyzed using an Olympus BX43 fluorescent microscope equipped with an Olympus DP74 digital camera (Olympus Corporation of the Americas, Center Valley, PA). At least 10 random fields from each slide were analyzed for staining intensity and localization. A semi-quantitative scale from 0 to 3+ was used to analyze the intensity of the staining, where 0 was absent, 1+ mild, 2+ moderate, and 3+ severe staining intensity. This analysis was performed by 1 nephropathologist who was blinded to the MS complement findings.

Urine Ba, C5a, and uMAC Measurements (Urine Cohort)

Urine Ba (uBa) levels were measured using a commercial anti-Ba enzyme-linked immunosorbent assay (ELISA) (Quidel Corporation, San Diego CA), according to the manufacturer's instructions.

Urine C5a (uC5a) was measured using an in-house sandwich ELISA as follows. Wells were coated with mouse anti-C5a antibody (clone 295003, R&D Systems, Minneapolis, MN) at 2 μg/ml. Urine samples diluted to 50% in 6% bovine serum albumin, 0.01 M phosphate buffer with 0.15 M NaCl (phosphate-buffered saline solution), and 0.015 M ethylenediamine tetraacetic acid (EDTA) were added and incubated for 1 hour at room temperature. Bound C5a was detected using biotinylated mouse anti-C5a (R&D Systems, clone 295009), and followed by streptavidin conjugated with biotin (R&D systems), and developed with 3,3′,5,5′-tetramethylbenzidine (TMB). A standard curve of purified C5a (Complement Technology, Tyler, TX) was used in each assay plate, and samples were normalized by urine creatinine (uCr) content. This ELISA had a lower limit of detection of 100 pg/ml urine and an interassay coefficient of variation of 3.9%. This ELISA was specific for free C5a, as shown by measuring the amount of C5a in plasma samples from 5 normal healthy individuals, where less than 1% of the amount of C5a in intact plasma C5 was detected.

The same general ELISA protocol described above was used to measure soluble uMAC, except that the coating antibody was a monoclonal specific for a neoepitope in the MAC (Quidel Corporation), and the detection antibody was a biotinylated rabbit polyclonal raised against soluble MAC (Complement Technology). This ELISA had a lower limit of detection of 12.5 ng/ml urine and an interassay coefficient of variation of 7.9%.

Statistical Analysis

The 3 groups (IgG4 pMN, IgG1 pMN, and control) were compared for differences in complement protein counts derived from the laser capture microdissection−MS/MS data. Peptides with raw spectral counts below 2 for at least 50% of samples of each group were removed, and normalization was applied to the observed spectral counts toward the common library size.[14] The Limma method with voom transformation[15] on the count data was used for modeling and testing for differential expression among groups. The *P*-value cut-offs were determined by controlling the mean number of false-positive results. Principal

Table 2. Mean spectral counts of PLA2R, complement proteins and complement system regulators

Protein detection	Accession no.	Mean spectral count (SD)		
		IgG1-MN	IgG4-MN	Control
Secretory phospholipase A2 receptor *OS = Homo sapiens GN = PLA2R1 PE = 1 SV = 2*	sp|Q13018|PLA2R_HUMAN	1.57 (3.31)	7.75 (3.75)	2.00 (1.41)
Cluster of Complement C1q subcomponent subunit C *OS = Homo sapiens GN = C1QC PE = 1 SV = 3*	sp|P02747|C1QC_HUMAN	1.43 (0.79)	1.25 (0.96)	0.00 (0.00)
Cluster of Complement C3 *OS = Homo sapiens GN = C3 PE = 1 SV = 2*	sp|P01024|CO3_HUMAN [2]	103.21 (25.19)	125.63 (24.26)	19.8 (5.06)
Cluster of Complement C4-B *OS = Homo sapiens GN = C4B PE = 1 SV = 2*	sp|P0C0L5|CO4B_HUMAN [2]	48.92 (24.59)	49.00 (13.55)	9.60 (5.67)
Complement C5 *OS = Homo sapiens GN = C5 PE = 1 SV = 4*	sp|P01031|CO5_HUMAN	25.00 (15.98)	27.00 (21.04)	1.40 (1.85)
Complement component C6 *OS = Homo sapiens GN = C6 PE = 1 SV = 3*	sp|P13671|CO6_HUMAN	9.93 (6.44)	7.75 (4.79)	1.40 (0.96)
Complement component C7 *OS = Homo sapiens GN = C7 PE = 1 SV = 2*	sp|P10643|CO7_HUMAN	5.07 (3.32)	4.75 (3.52)	0.20 (0.45)
Cluster of Complement component C8 beta chain *OS = Homo sapiens GN = C8B PE = 1 SV = 3*	sp|P07358|CO8B_HUMAN [2]	6.93 (3.76)	6.50 (4.04)	0.40 (0.55)
Complement component C8 gamma chain *OS = Homo sapiens GN = C8G PE = 1 SV = 3*	sp|P07360|CO8G_HUMAN	6.21 (4.41)	8.50 (6.49)	0.70 (1.09)
Complement component C9 *OS = Homo sapiens GN = C9 PE = 1 SV = 2*	sp|P02748|CO9_HUMAN	28.21 (18.00)	21.38 (14.94)	4.10 (2.46)
Complement receptor type 1 *OS = Homo sapiens GN = CR1 PE = 1 SV = 3*	sp|P17927|CR1_HUMAN (+1)	0.00 (0.00)	0.38 (0.75)	3.20 (1.82)
Cluster of Complement factor H *OS = Homo sapiens GN = CFH PE = 1 SV = 4*	sp|P08603|CFAH_HUMAN [2]	4.86 (2.32)	5.75 (3.07)	1.00 (0.94)
Cluster of Complement factor H-related protein 2 *OS = Homo sapiens GN = CFHR2 PE = 1 SV = 1*	sp|P36980|FHR2_HUMAN [4]	4.36 (2.39)	6.63 (4.42)	1.50 (1.12)
Vitronectin *OS = Homo sapiens GN = VTN PE = 1 SV = 1*	sp|P04004|VTNC_HUMAN	17.21 (7.89)	20.87 (10.18)	8.50 (1.58)
Cluster of Isoform 2 of Clusterin *OS = Homo sapiens GN = CLU*	sp|P10909-2|CLUS_HUMAN [3]	10.93 (5.89)	11.00 (5.87)	5.60 (2.19)

PLA2R, phospholipase A2 receptor.
Note: Mannose-binding lectin, ficolins, and collectin were not detected in kidney tissues by mass spectrometry.

component analysis and 2-way hierarchical clustering with heat maps were used for data exploration.

In the second cohort, correlations between urine complement component levels and complement components and proteinuria were calculated using the Pearson correlation test

RESULTS

Detection of pMN-Associated Podocyte Antigens by MS

IgG4-dominant MN had higher mean spectral counts of PLA2R compared to IgG1-dominant MN (Table 2). Interestingly, the IgG4-MN case with negative PLA2R by glomerular staining was positive by proteomic analysis, with a PLA2R mean spectral count of 4.5. THSD7A, Exotosin-1 and -2, and NELL-1 were not detected in any of these pMN biopsy specimens.

Detection of Glomerular Complement Proteins and Complement System Regulators by MS

Eight proteins of the complement pathway (C1q, C3, C4, C5, C6, C7, C8, and C9) and 5 complement regulators (complement receptor type 1[CR1], factor H [FH], FH-related protein 2 [FHR2], vitronectin, and clusterin) were differentially present in MN compared to controls. The total spectral counts for all complement proteins and complement regulators were comparable between IgG1- and IgG4-dominant MN (Table 2). In 3 of the IgG1-dominant MN cases, the glomerular capillary deposits had microspherical inclusions by electron microscopy, but the results in these cases were not different. A principal component analysis of glomerular complement proteins and complement regulators demonstrated clustering and separation of pMN patients and controls (Figure 1). The complement proteins C1q and C3−9 were more abundant in pMN than in healthy kidney (Table 3, Figure 2). CR1 was more abundant in healthy glomeruli, whereas all of the other complement regulatory proteins were more abundant in pMN (Table 3, Figure 2). Considering individual complement components, C3 had the highest spectral counts across all pMN patients.

Immunohistological Analysis of Kidney Biopsy Specimens

Immunofluorescence staining for C1q and C3 was routinely performed at the time of kidney biopsy. To mirror the MS findings that showed absent to minimal C1q and presence of C4d, suggestive of mannose-binding lectin pathway involvement, the immunohistological staining for complement component was supplemented in the MS pMN cohort by staining for C4d, mannan-binding lectin serine protease 1 (MASP-

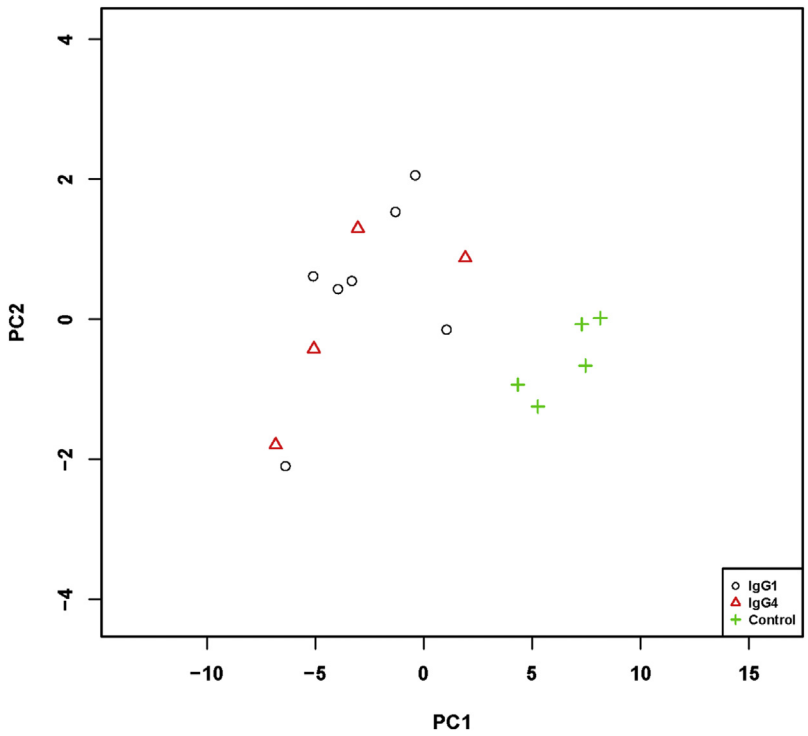

Figure 1. Principal component analysis of glomerular complement protein levels. Healthy controls clustered separately from membranous nephropathy (MN) patients. PC1 explained 87.6% of variation, and PC2 explained 4.5% of variation.

1), and mannan-binding lectin serine protease 2 (MASP-2) in all but 1 of the pMN cases (one IgG1-pMN specimen was not available for subsequent staining). Staining for M-ficolin, L-ficolin, and C5−9 were performed as well. All available pMN cases showed negative or trace staining for C1q, but were positive for C3 and C4 (Table 4, Supplementary Figure S1). All pMN cases stained positively for at least 1 component of the complement−lectin pathway (Table 4, Supplementary Figure S1).

Urine Excretion of Complement Activation Products

To look for evidence that the increased abundance of complement proteins in glomeruli of patients with pMN was associated with intrarenal complement activation, we measured uBa, generated when Factor B is cleaved; uC5a, generated when C5 is cleaved; and urine-soluble MAC, generated during terminal complement pathway activation. As shown in Table 5, uBa and uC5a were detected in all patients, and uMAC was present in 11 of 13 patients. The uBa correlated with uC5a and uMAC ($r = 0.87$ and 0.89; $P = 0.001$), and the uC5a levels correlated with uMAC ($r = 0.97$, $P = 0.001$). The uBa correlated with spot urine PCR (spot uPCR) ($r = 0.83$, $P = 0.001$). Also, uC5a and uMAC levels correlated with spot uPCR ($r = 0.66$ and $r = 0.69$, $P = 0.010$ and $P = 0.006$); however, the correlations were driven mainly by those with heaviest proteinuria.

DISCUSSION

In this study, we evaluated the presence and abundance of complement proteins in the glomeruli of patients with IgG4- and IgG1-dominant pMN using a proteomic approach. Although there were no significant differences in complement protein levels between IgG4- and IgG1-dominant pMN, the presence and abundance of complement components C1q and C3 to C9 in pMN was significantly greater than in healthy individuals. In addition, complement regulatory protein levels were similar in both pMN groups, but significantly higher than in healthy controls, except for CR1, which was lower in the pMN group. Coupled with the finding in a second active pMN cohort that C5a, Ba, and MAC were present in the majority of urine samples, these data support the involvement of the complement system in the pathogenesis of pMN.

These data are consistent with a recently published proteomic study of glomeruli isolated from kidney biopsy tissue of patients with PLA2R and EXT1/EXT2-associated MN that showed absent or minimal C1 and high spectral counts of complement proteins C3 to C9 in pMN.[16] Similarly, complement-regulating proteins were detected, and, in addition to those found by us, FHR-1, FHR-5, CD59, properdin, and FB were detected.

Importantly, the presence of these proteins in glomeruli does not by itself indicate that intrarenal complement activation is occurring. However, the

Table 3. Differentially detected complement proteins in all MN compared to normal controls

Complement component	Accession no.	All MN versus controls, fold change	*P* value
Cluster of Complement C1q subcomponent subunit C *OS = Homo sapiens GN = C1QC PE = 1 SV = 3*	sp|P02747|C1QC_HUMAN	3.39	1.3×10^{-6}
Cluster of Complement C3 *OS = Homo sapiens GN = C3 PE = 1 SV = 2*	sp|P01024|CO3_HUMAN [2]	8.68	3.2×10^{-10}
Cluster of Complement C4-B *OS = Homo sapiens GN = C4B PE = 1 SV = 2*	sp|P0C0L5|CO4B_HUMAN [2]	7.65	3.4×10^{-9}
Complement C5 *OS = Homo sapiens GN = C5 PE = 1 SV = 4*	sp|P01031|CO5_HUMAN	16.44	9.5×10^{-7}
Complement component C6 *OS = Homo sapiens GN = C6 PE = 1 SV = 3*	sp|P13671|CO6_HUMAN	5.60	1.1×10^{-4}
Complement component C7 *OS = Homo sapiens GN = C7 PE = 1 SV = 2*	sp|P10643|CO7_HUMAN	6.92	1.4×10^{-6}
Cluster of Complement component C8 beta chain *OS = Homo sapiens GN = C8B PE = 1 SV =3*	sp|P07358|CO8B_HUMAN [2]	7.79	3.7×10^{-6}
Complement component C8 gamma chain *OS = Homo sapiens GN = C8G PE = 1 SV = 3*	sp|P07360|CO8G_HUMAN	7.26	3.5×10^{-5}
Complement component C9 *OS = Homo sapiens GN = C9 PE = 1 SV = 2*	sp|P02748|CO9_HUMAN	6.81	5.6×10^{-5}
Complement receptor type 1 *OS = Homo sapiens GN = CR1 PE = 1 SV = 3*	sp|P17927|CR1_HUMAN (+1)	0.46	8.3×10^{-4}
Cluster of Complement factor H *OS = Homo sapiens GN = CFH PE = 1 SV = 4*	sp|P08603|CFAH_HUMAN [2]	5.04	2.6×10^{-5}
Cluster of Complement factor H-related protein 2 *OS = Homo sapiens GN = CFHR2 PE = 1 SV = 1*	sp|P36980|FHR2_HUMAN [4]	3.97	3.2×10^{-4}
Vitronectin *OS = Homo sapiens GN = VTN PE = 1 SV = 1*	sp|P04004|VTNC_HUMAN	3.10	2.6×10^{-4}
Cluster of Isoform 2 of Clusterin *OS = Homo sapiens GN = CLU*	sp|P10909-1|CLUS_HUMAN [3]	2.64	2.5×10^{-3}

MN, membranous nephropathy.

presence of the complement activation products C5a, Ba, and MAC in the urine is suggestive. Although uMAC correlated with proteinuria, the generation of MAC within the kidney during MN is reasonable based on its molecular weight, which, at around 1,000,000 Da, is likely too large to be filtered, even in nephrotic patients. An intrarenal origin of uC5a is less certain. C5a has a molecular weight of about 10,400 Da and is positively charged, so it can be freely filtered through the glomerular basement membrane. Although they were not tested in the current study, plasma C5a levels have been found to be elevated in patients with MN,[17] and uC5a also correlated with the magnitude of proteinuria in our pMN cohort. Nonetheless, if MAC is formed in the kidney, this would imply that C5 can also be cleaved within the kidney, given the dependence of MAC formation on C5 cleavage, and the strong correlation between uC5a and uMAC.

Complement can be activated through the classical, lectin, or alternative pathway. The presence of IgG1 in pMN, a strong C1q fixer, could certainly drive the classical pathway. Both galactose-deficient IgG1 and IgG4, and particularly anti-PLA2R antibodies, can initiate the lectin pathway.[18–20] Which, if either, pathway is involved in this cohort is unclear. Although glomerular C1q was found by MS in pMN, it was the least abundant of the complement proteins that were detected. On the other hand, neither mannose-binding lectin, ficolin, nor collectin, all lectin pathway activators, were detected by mass spectrometry. The immunofluorescence showed no C1q, but at least 1 of the lectin pathway components. The abundance of C4 by mass spectrometry and high C4d staining point to 1 or both of these pathways. The presence of Ba in the urine implies alternative pathway involvement. The presence of MAC in the urine indicates that this activation proceeded through the terminal pathway.

Mass spectrometry also showed the differential presence of a number of complement regulatory proteins in pMN glomeruli compared to control glomeruli. Whether they are negatively influencing the degree of intraglomerular complement activation is unclear. However, in this regard, CR1 was the 1 regulatory

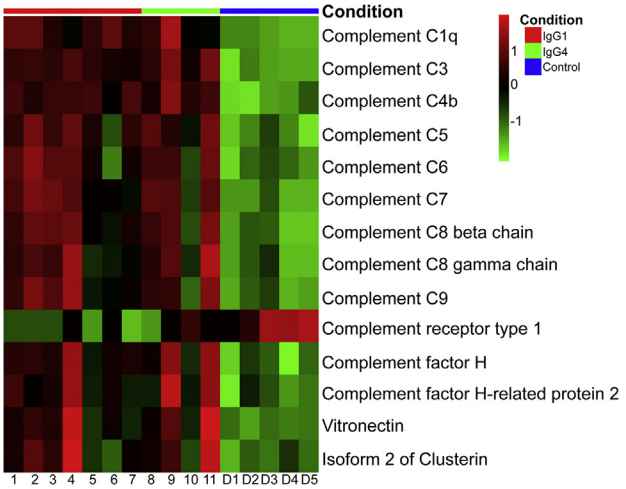

Figure 2. Heat map of glomerular complement protein abundance in primary membranous nephropathy (pMN) patients and healthy controls. Each column represents an individual patient with MN (1–11) or healthy control (D1–D5). Each row represents peptide spectral counts. Red represents higher protein expression and green lower protein expression. Scale −1 to 1 reflects relative protein expression re-scaled within each protein by centering at 0 and dividing by the SD.

Table 4. Glomerular immunohistological staining for complement components of kidney biopsy specimens from the mass spectrometry cohort

ID	MN-type	C1q	C3	C4d	M-Ficolin	L-Ficolin	MASP1	MASP2	C5b-9
1	IgG1	neg	1+ GCW	3+ GCW	Negative	Negative	neg	1+GCW	3+GCW
2	IgG1	neg	1+ GCW	2+ M	1+C	2+ GCW	neg	2+GCW	2+GCW
3	IgG1	neg	2+ Pod	3+ GCW	TR GCW, 2+pod	neg	1+GCW	1+GCW	2+GCW
4	IgG1	neg	1+GCW, 3+M	NA	NA	NA	NA	NA	NA
5	IgG1	TR M	2+ M	3+ GCW	neg	neg	neg	2+GCW	2+ GCW
6	IgG1	TR M	1+ PM	3+ GCW	1+ GCW	neg	neg	3+GCW	1+GCW
7	IgG1	neg	1+ GCW	3+ GCW	TR M,G	neg	1+GCW	3+GCW	2+ GCW
8	IgG4	neg	2+ GCW	2+ M	TRG, pod	neg	neg	3+GCW	3+GCW
9	IgG4	TR glom	TR GCW	3+ GCW	TR G	neg	1+GCW	3+GCW	3+GCW
10	IgG4	TR glom	1+ GCW	3+ GCW	1+ GCW,M	neg	1+GCW	3+GCW	2+GCW
11	IgG4	neg	3+ GCW	2+ M	TR GCW	neg	neg	3+GCW	3+GCW

C, cast; GCW, glomerular capillary wall; glom, glomerular; M, mesangial; MASP1, mannan-binding lectin serine protease 1; MASP2, mannan-binding lectin serine protease 2; MN, membranous nephropathy; NA, tissue not available for extra staining; neg, negative; PM, peri-mesangial; Pod, podocyte; TR, trace.

factor that was less abundant in pMN than in controls. The normal expression of CR1 in the kidney occurs on the podocyte, and, based on this expression site, it is tempting to propose that CR1 is critical to control complement regulation when the filtration barrier is compromised.[21] Loss of CR1 at the site of the damaged filtration barrier could significantly accelerate complement activation, which could in turn facilitate further damage to the barrier, leading to the high level of proteinuria characteristic of pMN.

There are limitations to this study. First, the number of patients assessed was small, both in the proteomic/immunohistological studies and in the urine measurements. Second, the cohort with proteomic and immunohistological data did not have available matching urine samples for C5a, Ba, and MAC analysis. Third, the complement activation products uBa, uC5a, and uC5b-9 correlate with proteinuria magnitude. This suggests either that the complement activation is contributing to kidney damage leading to proteinuria, or that the damage to the glomerular filtration barrier leading to proteinuria is causing complement activation. Although these are important questions of causality versus consequence (with or without contributing to disease progression), the current study was not designed to address this. Finally, the proteomic data do not indicate whether the complement proteins present in the pMN glomeruli are there because of glomerular expression or whether they are coming from the plasma during filtration, possibly through covalent binding as in the case of C3 and C4, or through strong membrane associations as in the case of C1q and the complement proteins in the form of the MAC (C5−9). Of relevance, *in situ* hybridization studies of a variety of glomerulopathies have shown the presence of C3 and C4 message in renal tubules, but not in

Table 5. Urine complement activation products from the "urine cohort"

Urine pMN cohort	PLA2R staining	Scr mg/dl	uCr mg/ml	uPCR g/g	uBα ng/mg uCr	uC5α ng/mg uCr	uMAC ng/mg uCr
Healthy control	Not done	0.90	2.00	0.00	8.00	0.00	0.00
Healthy control	Not done	NA	1.40	0.00	3.68	0.00	0.00
IgG4	Positive	1.50	0.92	10.00	10536.19	437.11	7880.44
IgG4	Positive	0.80	0.94	4.00	392.23	5.29	668.72
IgG4	Positive	1.00	1.23	2.60	61.14	0.73	128.05
IgG4	Positive	1.00	1.42	5.80	426.06	7.32	1546.55
IgG4	Positive	0.80	0.59	5.80	90.68	0.89	95.93
Co- dominant IgG4/IgG1	Weak	0.80	0.98	2.40	331.22	5.33	375.05
Co-dominant IgG4/IgG1	Negative	0.70	1.37	2.20	12.62	0.21	0.00
Co-dominant IgG4/IgG1	Positive	3.10	0.40	11.00	8000.00	97.00	1996.63
Co-dominant IgG4/IgG1	Positive	3.00	1.26	5.70	5926.19	82.00	2750.32
Co-dominant IgG4/IgG1	Positive	1.00	1.75	2.80	372.91	1.87	233.06
Co-dominant IgG4/IgG1	Negative	1.10	1.51	5.80	19.27	0.25	13.74
IgG1	Negative	1.30	0.67	4.00	14.92	0.17	0.00
IgG1	Weak	1.00	1.86	2.50	191.07	1.07	91.32
Mean value of complement activation products (SD) for the 13 MN patients					2028.81 (3620.03)	49.17 (121.06)	1213.83 (2190.25)

MN, membranous nephropathy; NA, not available; PLA2R, phospholipase A2 receptor, pMN, primary membranous nephropathy; Scr, serum creatinine; uCR, urine creatinine; uMAC, urine membrane attack complex or urine MAC; uPCR, urine protein/creatinine.

glomeruli.[22] Whether this suggest that the proteins identified in this study in the glomeruli of pMN patients indeed derive from another source (e.g., plasma), or suggests that pMN is unique with regard to intrarenal complement expression, remains to be determined.

In summary, inhibition of the complement system in pMN may be a reasonable adjunct to therapies designed to attenuate autoantibody (e.g., anti-PLA2R) production. We suggest that complement-targeted therapies may limit glomerular damage while waiting for autoantibody inhibition to take effect. Urine complement levels, specifically C5a, Ba, and MAC, may also be biomarkers of active MN, and could help differentiate patients who need treatment from patients who have proteinuria from chronic kidney injury.

DISCLOSURE

This was supported in part by an NIH NIDDK Grant: DK096927. BHR is a consultant for Morphosys and a consultant for Genentech (for MN treatment). All the other authors declare no competing interests.

SUPPLEMENTARY MATERIAL

Supplementary File (PDF)

Table S1. Antibodies for immunohistological staining.

Figure S1. Representative immunohistological staining.

REFERENCES

1. Hull RP, Goldsmith DJ. Nephrotic syndrome in adults. *BMJ*. 2008;336(7654):1185–1189.
2. Glassock RJ. Diagnosis and natural course of membranous nephropathy. *Semin Nephrol*. 2003;23:324–332.
3. Beck LH Jr, Bonegio RG, Lambeau G, et al. M-type phospholipase A2 receptor as target antigen in idiopathic membranous nephropathy. *N Engl J Med*. 2009;361:11–21.
4. Tomas NM, Beck LH Jr, Meyer-Schwesinger C, et al. Thrombospondin type-1 domain-containing 7A in idiopathic membranous nephropathy. *N Engl J Med*. 2014;371:2277–2287.
5. Sethi S, Debiec H, Madden B, et al. Neural epidermal growth factor-like 1 protein (NELL-1) associated membranous nephropathy. *Kidney Int*. 2020;97:163–174.
6. Caza T, Hassen S, Dvanajscak Z, et al. NELL1 is a target antigen in malignancy-associated membranous nephropathy [epub ahead of print]. *Kidney Int*. https://doi.org/10.1016/j.kint.2020.07.039. Accessed October 28, 2020.
7. Ponticelli C, Glassock RJ. Glomerular diseases: membranous nephropathy—a modern view. *Clin J Am Soc Nephrol*. 2014;9:609–616.
8. Imai H, Hamai K, Komatsuda A, et al. IgG subclasses in patients with membranoproliferative glomerulonephritis, membranous nephropathy, and lupus nephritis. *Kidney Int*. 1997;51:270–276.
9. Ohtani H, Wakui H, Komatsuda A, et al. Distribution of glomerular IgG subclass deposits in malignancy-associated membranous nephropathy. *Nephrol Dial Transplant*. 2004;19:574–579.
10. Kuroki A, Shibata T, Honda H, et al. Glomerular and serum IgG subclasses in diffuse proliferative lupus nephritis, membranous lupus nephritis, and idiopathic membranous nephropathy. *Intern Med*. 2002;41:936–942.
11. Sethi S, Madden BJ, Debiec H, et al. Exostosin 1/exostosin 2-associated membranous nephropathy. *J Am Soc Nephrol*. 2019;30:1123–1136.
12. Salant DJ. Unmet challenges in membranous nephropathy. *Curr Opin Nephrol Hypertens*. 2019;28:70–76.
13. Nesvizhskii AI, Keller A, Kolker E, Aebersold R. A statistical model for identifying proteins by tandem mass spectrometry. *Anal Chem*. 2003;75:4646–4658.
14. Robinson MD, Oshlack A. A scaling normalization method for differential expression analysis of RNA-seq data. *Genome Biol*. 2010;11:R25.
15. Law CW, Chen Y, Shi W, Smyth GK. voom: Precision weights unlock linear model analysis tools for RNA-seq read counts. *Genome Biol*. 2014;15:R29.
16. Ravindran A, Madden B, Charlesworth MC, et al. Proteomic analysis of complement proteins in membranous nephropathy. *Kidney Int Rep*. 2020;5:618–626.
17. Zhang MF, Huang J, Zhang YM, et al. Complement activation products in the circulation and urine of primary membranous nephropathy. *BMC Nephrol*. 2019;20:313.
18. Malhotra R, Wormald MR, Rudd PM, et al. Glycosylation changes of IgG associated with rheumatoid arthritis can activate complement via the mannose-binding protein. *Nature Med*. 1995;1:237–243.
19. Salant DJ. Genetic variants in membranous nephropathy: perhaps a perfect storm rather than a straightforward conformeropathy? *J Am Soc Nephrol*. 2013;24:525–528.
20. Haddad G, Kistler A. An in vitro model of idiopathy membranous nephropathy reveals PLA2R- and complement-dependent pathways of podocyte injury. *J Am Soc Nephrol*. 2017;20:109A.
21. Mathern DR, Heeger PS. Molecules great and small: the complement system. *Clin J Am Soc Nephrol*. 2015;10:1636–1650.
22. Welch TR, Beischel LS, Witte DP. Differential expression of complement C3 and C4 in the human kidney. *J Clin Invest*. 1993;92:1451–1458.